Hippocampus

	B16F10 IgG	**B16F10 PD-1**	**B16F10 PD-L1**	**MC38 IgG**	**MC38 PD-1**	**MC38 PD-L1**
Gene Symbol	2^-ΔCT (Mean ± SEM)	2^-ΔCT (Mean ± SEM), p-value	2^-ΔCT (Mean ± SEM), p-value	2^-ΔCT (Mean ± SEM)	2^-ΔCT (Mean ± SEM), p-value	2^-ΔCT (Mean ± SEM), p-value
ARG1	0.0067445 ± 0.0009431	0.0149475 ± 0.0075884 p=0.50	0.0090549 ± 0.0017240 P>0.99	0.0133699 ± 0.0050632	0.0093781 ± 0.0020925 p=0.93	0.0082522 ± 0.0025193 p=0.84
CCL2	0.0013763 ± 0.0002147	0.0012922 ± 0.0002143 p>0.99	0.0017097 ± 0.0002934 p>0.99	0.0007517 ± 0.0002371	0.0004132 ± 0.0001189 p>0.99	0.0005801 ± 0.0001663 p>0.99
CCL19	**0.0003817 ± 0.0000590**	0.0013981 ± 0.0009603 p=0.97	0.0004324 ± 0.0000484 p=0.99	0.0006364 ± 0.0002694	**0.0093781 ± 0.0020925 ***, p=0.0003**	**0.0082522 ± 0.0025193 **, p=0.002**
CCL21	0.0000267 ± 0.0000096	0.0001074 ± 0.0000789 p>0.99	0.0000492 ± 0.0000125 p>0.99	0.0001588 ± 0.0000603	0.0019292 ± 0.0018877 p>0.99	0.0046654 ± 0.0046281 p=0.95
CD4	0.0002682 ± 0.0000288	0.0018002 ± 0.0015978 p=0.80	0.0002816 ± 0.0000515 p>0.99	0.0017776 ± 0.0011500	0.0002997 ± ± 0.0000611 p=0.86	0.0004333 0.0000911 p>0.99
CD8A	0.0000578 ± 0.0000162	0.0004255 ± 0.0003614 p>=0.99	0.0000763 ± 0.0000292 p>0.99	0.0001661 ± 0.0001237	0.0000813 ± 0.0000192 p>0.99	0.0000990 ± 0.0000406 p>0.99
CD8B	0.0028036 ± 0.0015292	0.0018914 ± 0.0006171 p>0.99	0.0012733 ± 0.0005952 p>0.99	0.0025207 ± 0.0011346	0.0012208 ± 0.0002994 p>0.99	0.0009680 ± 0.0003293 p=0.60
ITGAM (CD11b)	0.0415633 ± 0.0068409	0.0378463 ± 0.0041501 p>0.99	0.0440255 ± 0.0039618 p>0.99	0.0244942 ± 0.0042802	0.0337442 ± 0.0062526 p=0.87	0.0216065 ± 0.0050506 p>0.99
ITGAX (CD11c)	0.0000406 ± 0.0000164	0.0003735 ± 0.0003488 p>0.99	0.0000602 ± 0.0000246 p>0.99	0.0038039 ± 0.0036618	0.0000879 ± 0.0000216 p=0.50	0.0000719 ± 0.0000248 p=0.62
CD14	0.0055400 ± 0.0007871	0.0269412 ± 0.0211175 p>0.99	0.0071636 ± 0.0022949 p>0.99	0.0266960 ± 0.0144054	0.0087711 ± 0.0019387 p=0.99	0.0063844 ± 0.0019771 p=0.91
CD19	0.0051376 ± 0.0011001	0.0039557 ± 0.0006161 p>0.99	0.0052230 ± 0.0004111 p>0.99	0.0029670 ± 0.0008266	0.0034033 ± 0.0006155 p>0.99	0.0030622 ± 0.0006975 p>0.99
CD80	0.0003818 ± 0.0000809	0.0003344 ± 0.0000566 p>0.99	0.0003589 ± 0.0000384 p>0.99	0.0001773 ± 0.0000649	0.0003462 ± 0.0000515 p=0.25	0.0003015 ± 0.0000613 p=0.66

CD86	0.0009511 ± 0.0001611	0.0007966 ± 0.0001741 p>0.99	0.0011831 ± 0.0001514 p>0.99	0.0020223 ± 0.0012258	0.0051437 ± 0.0030561 p>0.99	0.0014088 ± 0.0003630 p>0.99
CGAS	0.0005005 ± 0.0000572	0.0004475 ± 0.0000856 ± p>0.99	0.0005190 ± 0.0000718 p>0.99	0.0003034 ± 0.0000499	0.0003657 ± 0.0000738 p>0.99	0.0004359 ± 0.0000862 p=0.88
CHI3L3	0.0024243 ± 0.0004485	0.0042919 0.0023536 p>0.99	0.0028082 ± 0.0003072 p>0.99	0.0026799 ± 0.0008343	0.0026339 ± 0.0005533 p>0.99	0.0022969 ± 0.0005736 p>0.99
CSF1	Undetermined	Undetermined	Undetermined	Undetermined	Undetermined	Undetermined
CSF2	0.0001970 ± 0.0000397	0.0003031 ± 0.0000818 p>0.99	0.0002092 ± 0.0000395 p>0.99	0.0016664 ± 0.0014915	0.0002997 ± 0.0000759 p=0.62	0.0001734 ± 0.0000523 p=0.56
CXCL12	0.0021006 ± 0.0002500	0.0035411 ± 0.0007081 p=0.44	0.0021131 ± 0.0003000 p>0.99	0.0034343 ± 0.0010051	0.0077324 ± 0.0040751 p>0.99	0.0044830 ± 0.0018730 p>0.99
CX3CL1	0.0409684 ± 0.0047587	0.0441273 ± 0.0024195 p>0.99	0.0422356 ± 0.0014890 p>0.99	0.0280336 ± 0.0036311	0.0523864 ± 0.0135968 p=0.36	0.0368849 ± 0.0106001 p>0.99
FOXP3	0.0000664 ± 0.0000225	0.0002107 ± 0.0001635 p>0.99	0.0000632 ± 0.0000182 p>0.99	0.0068721 ± 0.0067988	0.0001395 ± 0.0000564 p=0.30	0.0000718 ± 0.0000215 p>0.99
INFG	0.0580796 ± 0.0061225	0.1261078 ± 0.0582322 p=0.32	0.0733725 ± 0.0121845 p>0.99	0.0797533 ± 0.0124105	0.0970576 ± 0.0139338 p>0.99	0.0602412 ± 0.0145605 p>0.99
IL1A	0.0001029 ± 0.0000342	0.0000846 ± 0.0000237 p>0.99	0.0000817 ± 0.0000233 p>0.99	0.0000382 ± 0.0000075	0.0001669 ± 0.0000990 p>0.99	0.0001352 ± 0.0000913 p>0.99
IL1B	0.0015101 ± 0.0002277	0.0023820 ± 0.0008399 p>0.99	0.0016860 ± 0.0002187 p>0.99	0.0066885 ± 0.0044030	0.0019082 ± 0.0005565 p=0.25	0.0014162 ± 0.0003448 p=0.17
IL2	0.0031988 ± 0.0003246	0.0063271 ± 0.0022036 p=0.16	0.0041177 ± 0.0004506 p>0.99	0.0039404 ± 0.0004708	0.0046377 ± 0.0004423 p>0.99	0.0034795 ± 0.0007367 p>0.99
IL4	Undetermined	Undetermined	Undetermined	Undetermined	Undetermined	Undetermined
IL6	0.0002311 ± 0.0000407	0.0104853 ± 0.0097558 p=0.09	0.0003881 ± 0.0000480 p=0.78	0.0113390 ± 0.0078921	0.0012540 ± 0.0006164 p>0.99	0.0005991 ± 0.0001503 p=0.54
IL10	0.0987414 ± 0.0165440	0.0737602 ± 0.0135242	0.1270429 ± 0.0234479 p>0.99	0.0780419 ± 0.0190012	0.1216931 ± 0.0210763 p=0.49	0.0970067 ± 0.0210041 p>0.99

		p>0.99				
IL12	0.6087308 ± 0.0612123	0.7615834 ± 0.0643774 p>0.99	0.6868139 ± 0.0817340 p>0.99	0.4945699 ± 0.1208605	0.5754466 ± 0.1429042 p>0.99	0.4159060 ± 0.1324806 p>0.99
IL17	0.0014363 ± 0.0002551	0.0035135 ± 0.0017572 p=0.87	0.0018372 ± 0.0002799 p>0.99	0.0120318 ± 0.0096357	0.0021370 ± 0.0004428 p>0.99	0.0036143 ± 0.0009588 p>0.99
IL23A	0.0001155 ± 0.0000150	0.0007040 ± 0.0005614 p=0.90	0.0001620 ± 0.0000139 p=0.85	0.0002665 ± 0.0001403	0.0002124 ± 0.0000368 p>0.99	0.0012641 ± 0.0009168 p>0.99
LTA	0.0000291 ± 0.0000058	0.0001227 ± 0.0000695 p=0.60	0.0000561 ± 0.0000221 p>0.99	0.0000645 ± 0.0000269	0.0000731 ± 0.0000225 p>0.99	0.0000554 ± 0.0000180 p>0.99
LTB	0.0378029 ± 0.0044104	0.0810215 ± 0.0236368 p=0.85	0.0447666 ± 0.0079945 p>0.99	0.1217781 ± 0.0463359	0.0681839 ± 0.0220509 p=0.50	0.0375644 ± 0.0147469 **p=0.07**
MRC1	0.0064997 ± 0.0013135	0.0130289 ± 0.0066500 p>0.99	0.0090020 ± 0.0018591 p>0.99	0.0102726 ± 0.0018829	0.0126278 ± 0.0030638 p>0.99	0.0077288 ± 0.0018462 p>0.99
NOS2	0.0252442 ± 0.0038579	0.0251138 ± 0.0039587 p>0.99	0.0313684 ± 0.0049393 p>0.99	0.0240401 ± 0.0063295	0.0297323 ± 0.0038780 p>0.99	0.0249036 ± 0.0047086 p>0.99
PD1	0.0050931 ± 0.0010406	0.0259486 ± 0.0212001 p>0.99	0.0065762 ± 0.0018970 p>0.99	0.0159212 ± 0.0072419	0.0095585 ± 0.0013903 p>0.99	0.0050935 ± 0.0021159 p>0.99
PDL1	0.0066205 ± 0.0008299	0.0148009 ± 0.0076520 p>0.99	0.0077951 ± 0.0007904 p>0.99	0.0149422 ± 0.0080101	0.0108187 ± 0.0023389 p=0.88	0.0045456 ± 0.0017148 p=0.79
P2RY12	0.0001077 ± 0.0000362	0.0008682 ± 0.0008048 p>0.99	0.0002776 ± 0.0001720 p>0.99	0.0028472 ± 0.0024862	0.0103421 ± 0.0099846 p=0.43	0.0127510 ± 0.0126528 p>0.99
RORC	0.0005961 ± 0.0000850	0.0006956 ± 0.0001581 p>0.99	0.0007241 ± 0.0001105 p>0.99	0.0051008 ± 0.0044991	0.0009648 ± 0.0001702 p=0.48	0.0007334 ± 0.0001535 p=0.41
STING1	0.0111267 ± 0.0012241	0.0191055 ± 0.0040668 p=0.12	0.0124083 ± 0.0011101 p>0.99	0.0156044 ± 0.0029564	0.0113495 ± 0.0023295 p=0.94	0.0089138 ± 0.0019543 p=0.26
TGFB	0.0000225 ± 0.0000029	0.0005618 ± 0.0005300 p>0.99	0.0000471 ± 0.0000149 p>0.99	0.0003128 ± 0.0001555	0.0012359 ± 0.0009908 p>0.99	0.0002796 ± 0.0001444 p>0.99
TLR2	0.0000945 ± 0.0000239	0.0013860 ±	0.0002029 ± 0.0001168	0.0004897 ±	0.0006134 ± 0.0003254	0.0002207 ± 0.0000364

		0.0013206 p>0.99	p>0.99	0.0003056	p>0.99	p>0.99
TLR4	0.0003838 ± 0.0000848	0.0004083 ± 0.0000892 p>0.99	0.0005238 ± 0.0001666 p>0.99	0.0069910 ± 0.0047787	0.0016497 ± 0.0007895 p>0.99	0.0006330 ± 0.0001757 p>0.99
TNFA	0.0001947 ± 0.0000462	0.0002652 ± 0.0000805 p>0.99	0.0001916 ± 0.0000291 p>0.99	0.0020737 ± 0.0018562	0.0005064 ± 0.0003262 p>0.99	0.0004869 ± 0.0002938 p>0.99
TREMP2	0.0046420 ± 0.0007359	0.0048172 ± 0.0010888 p>0.99	0.0058668 ± 0.0004943 p=0.66	0.0042815 ± 0.0012343	0.0072111 ± 0.0018029 p>0.99	0.0063665 ± 0.0019738 p>0.99
VEGFC	0.0445284 ± 0.0046409	0.0385082 ± 0.0064324 p>0.99	0.0525114 ± 0.0151911 p>0.99	0.0269912 ± 0.0063351	0.0226125 ± 0.0074847 p>0.99	0.0219480 ± 0.0054654 p>0.99

Table S1. mRNA transcript levels of neuroinflammatory genes in the dura mater meningeal layer of cancer-bearing mice treated or not with immune check point inhibitors. Quantitative RT-PCR analysis of inflammatory gene expression in isolated meninges. Data are expressed as mean ± SEM of 2^-ΔCT where $\Delta CT = Ct_{target} - Ct_{ACTB}$. ACTB (*beta-actin*) was used as the reference gene (n = 3-7). Statistical analyses were performed by One-way ANOVA with Dunnett' or Sidak's multiple comparisons test or Kruskal-Wallis with Dunn's multiple comparisons test. Significantly modified genes are in bold.

Antibody	Purchaser	Dilution	Host	Reference
CD206	R&D systems	1:1000	goat	AF2535
MHCII	Invitrogen	1:1000	rat	14-5321-82
Cd11b	Abcam	1:200	rabbit	ab133357
Gr1	Fisher Scientific	1:500	rat	14-5931-85
Collagen IV	Novus Biologicals	1:1000	rabbit	NB120-6586
Meca-79	Santa Cruz	1:100	rat	sc-19602
PD-L1	Abcam	1:500	rabbit	AB213480-1001
CD8	Abcam	1:100	rat	ab22378
ICAM-1	Abcam	1:500	rat	ab25375
Lectin-Tl Fluorescein	Vector laboratories	1:200		FL1171
Madcam-1	Santa Cruz	1:500	rat	sc-19604
F4/80	Abcam	1:100	rabbit	ab111101
Podocalyxin	R&D Systems	1:1000	rat	MAB1556
BrDu	Abcam	1:1000	sheep	ab1893
NeuN	Abcam	1:1000	rabbit	ab104225
CD68	Invitrogen	1:500	rat	MA516674
Iba1	Wako	1:1000	rabbit	019-19741
Ki67	Fisher Scientific	1:1000	rat	14-5698-82
CCl19	Invitrogen	1:100	rabbit	PA5109488
CD3	R&D Systems	1:100	rat	MAB4841
Laminin	Sigma	1:1000	rabbit	L9393
TCRγδ	Invitrogen	1:100	hamster	14-5711-85
GFAP	Abcam	1:500	goat	ab53554
Arg-1	Santa Cruz	1:500	mouse	sc-271430
PD-1	Invitrogen	1:500	rabbit	PA5-20351
NeuN	Abcam	1:1000	mouse	ab104224
IGg2a	Novus Biologicals	1:200	goat	NBP2-69581
Donkey anti-rabbit DAR 488	Invitrogen	1:1000	Donkey	A21206
Donkey anti-goat DAG 488	Invitrogen	1:1000	Donkey	A11055
Donkey anti-sheep DAS 488	Invitrogen	1:1000	Donkey	A11015
Goat anti-hamster GAH 488	Invitrogen	1:1000	Donkey	A21110
Donkey anti-mouse DAM 488	Invitrogen	1:1000	Donkey	ab96875
Donkey anti-goat DAG 555	Invitrogen	1:1000	Donkey	A21432
Donkey anti-rabbit DAR 555	Invitrogen	1:1000	Donkey	A31572
Donkey anti-rat DARat IgG h&l Alexa fluor 647 preadsorbed	Abcam	1:1000	Donkey	AB150155-1001

Table S2. List of the used antibodies and related references.

Symbol	Name	Forward	Reverse
ACTB	Actin.beta	AGGTCATCACTATTGGCAACGA	CACAGGATTCCATACCCAAGAAG
ARG1	Arginase 1	GAAAGTTCCCAGATGTACCAGGAT	AATGTACACGATGTCTTTGGCAGAT
CCL2	Chemokine (C-C motif) ligand 2	AAGCTGTAGTTTTTGTCACCAAGCT	TTGGTTCCGATCCAGGTTTTTA
CCL19	Chemokine (C-C motif) ligand 19	GCATCATCCGAAGACTGAAGAA	TTTACTCAAGACACAGGGCTCCTT
CCL21	Chemokine (C-C motif) ligand 21	GGGAACCTCTAAGTCTGGAAAGAA	CGTGAACCACCCAGCTTGA
CD4	CD4 antigen	CTCTGAGGAGCAGAAAGTAGTTCAAG	CCAGGAACACTGTCTGGTTCAC
CD8A	CD8a antigen	AAATGTCCCAGGCCGCTAGT	GCGGTGCCATTTTACACAATT
CD8B	CD8b antigen	CGAAGCTGACTGTGGTTGATGT	TTCATCTTCAGGGTAGTCTTCTTGGT
ITGAM	ITGAM antigen	TCATCAACACAACCAGAGTGGATT	AGGTGCTCCTAAAACCAAGCTTT
ITGAX	ITGAX antigen	TGATAGTTCCTGGGTGGTGGTT	TGTAGAGGCCACCTATTTGGTTAGT
CD14	CD14 antigen	GCCTTTCTCGGAGCCTATCTG	CAACAGCAACAAGCCAAGCA
CD19	CD19 antigen	CTGTATGGTTTCTCTGGTGGCTTT	GTCATTCGCTTCCTTTTCCTTCT
CD80	CD80 antigen	AATAACAGTCGTCGTCATCGTTGT	CTGCTTGCCTCATTTCTTCTGA
CD86	CD86 antigen	TGTGGCATATGACCGTTGTGT	TCTTGAGTGAAATTGAGAGGTTTGG
CGAS	Cyclic GMP-AMP Synthase	GAGGCGCGGAAAGTCGTAA	TTGTCCGGTTCCTTCCTGGA
CHIL3	Chil3 - chitinase-like 1	AGATCACTTACACACATGAGCAAGACT	TCAGTGTTCTTGTCTTTCAGACCAT
CSF1	Colony stimulating factor 1	CCAAGGAGGTGTCAGAACACTGT	AAAGGCAATCTGGCATGAAGTC
CSF2	Colony stimulating factor 2	CAGCCAGCTACTACCAGACATACTG	CGCATAGGTGGTAACTTGTGTTTC
CXCL12	Chemokine (C-X-C motif) ligand 12	CTGTGCCCTTCAGATTGTTG	TAATTTCGGGTCAATGCACA
CX3CL1	C-X3-C Motif Chemokine Ligand 1	ACGAATCCCAGTGGCTTTGC	GTGTCGTCTCCAGGACAATGG
FOXP3	Forkhead box P3	TTTACTCGCATGTTCGCCTACTT	CTCAAATTCATCTACGGTCCACACT
IFNG	Interferon gamma	ATGAACGCTACACACTGCATC	CCATCCTTTTGCCAGTTCCTC
IL1A	Interleukin 1 alpha	GCACCTTACACCTACCAGAGT	AAACTTCTGCCTGACGAGCTT
IL1B	Interleukin 1 beta	GAAGAAGAGCCCATCCTCTGT	TGTTCATCTCGGAGCCTGTA
IL2	Interleukin 2	CAGGATGCTCACCTTCAAATTTTAC	CGCAGAGGTCCAAGTTCATCT
IL4	Interleukin 4	GAGAGAGATCATCGGCATTTTGA	TTCGTTGCTGTGAGGACGTTT
IL6	Interleukin 6	ACTCCCAACAGACCTGTCTATACCA	TGCCATTGCACAACTCTTTTCT
IL10	Interleukin 10	ATAAGCTCCAAGACCAAGGTGTCT	ACACACTGCAGGTGTTTTAGCTTTT
IL12	Interleukin 12	AGACATCACACGGGACCAAAC	CCAGGCAACTCTCGTTCTTGT

IL17	Interleukin 17	GGAGAGCTTCATCTGTGTCTCTGA	ATCGCTGCTGCCTTCACTGT
IL23A	Interleukin 23	CCAGCGGGACATATGAATCTACT	TCACAACCATCTTCACACTGGAT
LTA	Lymphotoxin Alpha	CACTTGACCCATGGCATCCT	GTTGCTCAAAGAGAAGCCATGTC
LTB	Lymphotoxin Beta	GGGAACCAGAAACTGACCTCAA	CGCTCCTCAGAAACGCTTCTT
MRC1	Mannose receptor. C type 1	GAGGGAAGCGAGAGATTATGGA	GCCTGATGCCAGGTTAAAGCA
NOS2	Nitric oxide synthase 2. inducible Gene	GGGCTGTCACGGAGATCA	CCATGATGGTCACATTCTGC
PD1	Programmed Cell Death 1	AGCTCGTGGTAACAGAGAGAATCC	AGGGCACTCATGATACCAATGA
PDL1	Programmed cells death ligand 1	GCTGGATCCACGGAAATTCTC	TGCGGACTACAAGCGAATCA
P2RY12	Purinergic receptor P2Y. G-protein coupled 12	GAACGCCTGCCTTGATCCAT	TGGTTCGCCACCTTCTTGTC
RORC	RAR-related orphan receptor gamma	CCATATTTGACTTTTCCCACTTCCT	GCAGATGTTCCACTCTCCTCTTC
STING1	Stimulator of interferon response cGAMP interactor 1	GGTCACCGCTCCAAATATGTAG	CAGTAGTCCAAGTTCGTGCGA
TGFB	Transforming growth factor. beta 1	TGGAGCAACATGTGGAACTC	CAGCAGCCGGTTACCAAG
TLR2	Toll-like receptor 2	GAATTGCATCACCGGTCAGAA	CCTCTGAGATTTGACGCTTTGTC
TLR4	Toll- like receptor 4	TTCTTCTCCTGCCTGACACCA	GGAATGTCATCAGGGACTTTGC
TNFA	Tumor necrosis factor alpha	CACCGTCAGCCGATTTGC	TGAGTTGGTCCCCCTTCTCC
TREMP2	Triggering receptor expressed on myeloid cells 2	TTCAGATCCTCACTGGACCC	CCTGGCTGGACTTAAGCTGT
VEGFC	Vascular endothelial growth factor C	GCATGAACACCAGCACAGGTTA	GCCTTGTGAGAGAGGCACTGTAAT

Table S3. List of couples of primers used for quantitative PCR.

a

Correlations between vascular and immune markers

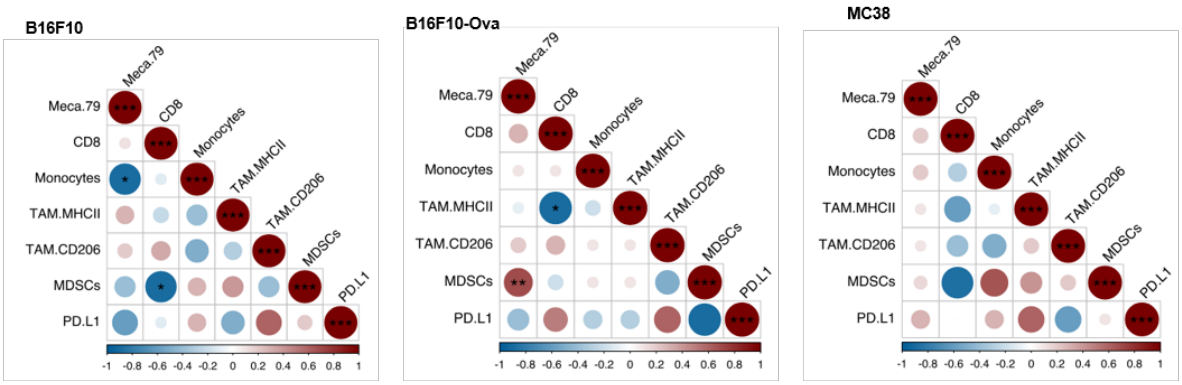

b

Immunoscore

Treatment	$CD8^+$ cells ($n/\mu m^2$)	Score	HEVs ($MECA79^+$ cells, % of total area)	Score	Monocytes ($CD11b^+GR1^-$ cells · n/mm^2)	Score	$MHCII^+$ cells (n/mm^2)	Score	Immunoscore
B16F10	9.013	0	0.960	0	72.100	1	72.101	0	**1**
	6.008	0	3.005	1	36.050	0	130.683	1	**2**
	12.017	1	3.270	2	18.025	0	78.860	0	**3**
	12.017	1	1.660	0	45.063	0	114.911	0	**1**
	12.017	1	2.080	0	54.070	1	90.126	0	**2**
B16F10-Ova	24.034	2	3.210	1	207.290	2	207.290	1	**6**
	12.017	1	4.856	3	351.400	3	259.113	1	**8**
	15.021	2	2.947	1	216.302	2	196.024	1	**6**
	0.000	0	3.113	1	36.050	0	459.643	3	**4**
	3.004	0	1.250	0	261.360	3	416.833	2	**5**
MC38	75.105	3	5.470	3	234.320	2	414.580	2	**10**
	45.063	3	5.720	3	243.340	2	351.492	2	**10**
	51.072	3	3.450	2	171.230	1	259.113	1	**7**
	27.038	2	3.770	2	360.500	3	585.820	3	**10**
	30.042	2	4.136	2	126.176	1	675.946	3	**8**
Score									
Maximum	75.105	3	5.720	3	360.500	3	675.946	3	
75% percentile	30.042		4.136		243.340		416.833		
75% percentile	30.042	2	4.136	2	243.340	2	416.833	2	
Median	12.017		3.210		171.230		259.113		
Median	12.017	1	3.210	1	171.230	1	259.113	1	
25% percentile	9.013		2.080		45.063		114.911		
25% percentile	9.013	0	2.080	0	45.063	0	114.911	0	
Minimum	0.000		0.960		18.025		72.101		

c

Immunosuppressive Score

Treatment	PD-L1 (% of total cells)	Score	MDSCs (n/mm^2)	Score	CD206 (n/mm^2)	Score	Immunosuppressive score
B16F10	94.620	3	126.177	2	423.593	2	7
	88.050	1	180.252	3	419.087	2	6
	88.660	1	81.114	1	675.946	3	5
	91.190	2	117.164	2	648.908	3	7
	67.660	1	99.139	2	225.315	0	3
B16F10-Ova	96.610	3	135.189	2	430.352	3	8
	91.620	2	234.328	3	351.492	1	6
	93.690	2	153.214	3	247.847	0	5
	92.410	2	162.227	3	254.606	1	6
	94.790	3	63.088	1	414.580	2	6
MC38	38.050	1	18.025	0	123.923	0	1
	13.800	0	45.063	1	344.732	1	2
	10.320	0	18.025	0	259.113	1	1
	15.890	0	54.076	1	180.252	0	1
	14.780	0	36.050	0	403.314	2	2
Score							
Maximum	96.610	3	234.320	3	675.946	3	
75% percentile	93.690		153.210		423.593		
75% percentile	93.690	2	153.210	2	423.593	2	
Median	88.660		99.138		351.492		
Median	88.660	1	99.138	1	351.492	1	
25% percentile	15.890		45.063		247.847		
25% percentile	15.890	0	45.063	0	247.847	0	
Minimum	10.320		18.025		123.923		

Figure S1. Marker labeling to calculate immune- and immune-suppressive scores. a. Correlation between immunostaining items used to define immunoscore and immunosuppressive score. Heatmap of

Kendall correlation coefficients; only significant correlations (* $p<0.05$; *** $p<0.0001$) are displayed (adjusted p-value <0.05) and values obtained in B16F10, B16F10-Ova and MC38 have been pooled. **b.** Tables recapitulating the immunoscore calculation methods in B16F10, B16F10-Ova and MC38 tumor slices. Densities of $CD8^+$ TLs, Meca-79^+ HEVs, $CD11b^+$ monocytes and $MHCII^+$ pro-inflammatory TAMs in tumors were converted into percentile values. **c.** Table recapitulating the immunosuppressive score calculation methods in B16F10, B16F10-Ova and MC38 tumor slices. Densities of $CD206^+$ pro-tumoral TAMs, $CD11b^+GR1^+$ MDSCs and percentage of PD-$L1^+$ cells in tumors were converted into percentile values. **b and c.** Percentiles values were converted into score values with score 0 attributed to percentile values ranking from (0-25%), score 1 (25-50%), score 2 (50-70%), score 3 (75-100%). The mean of each score was then calculated to generate immunoscore or immunosuppressive score.

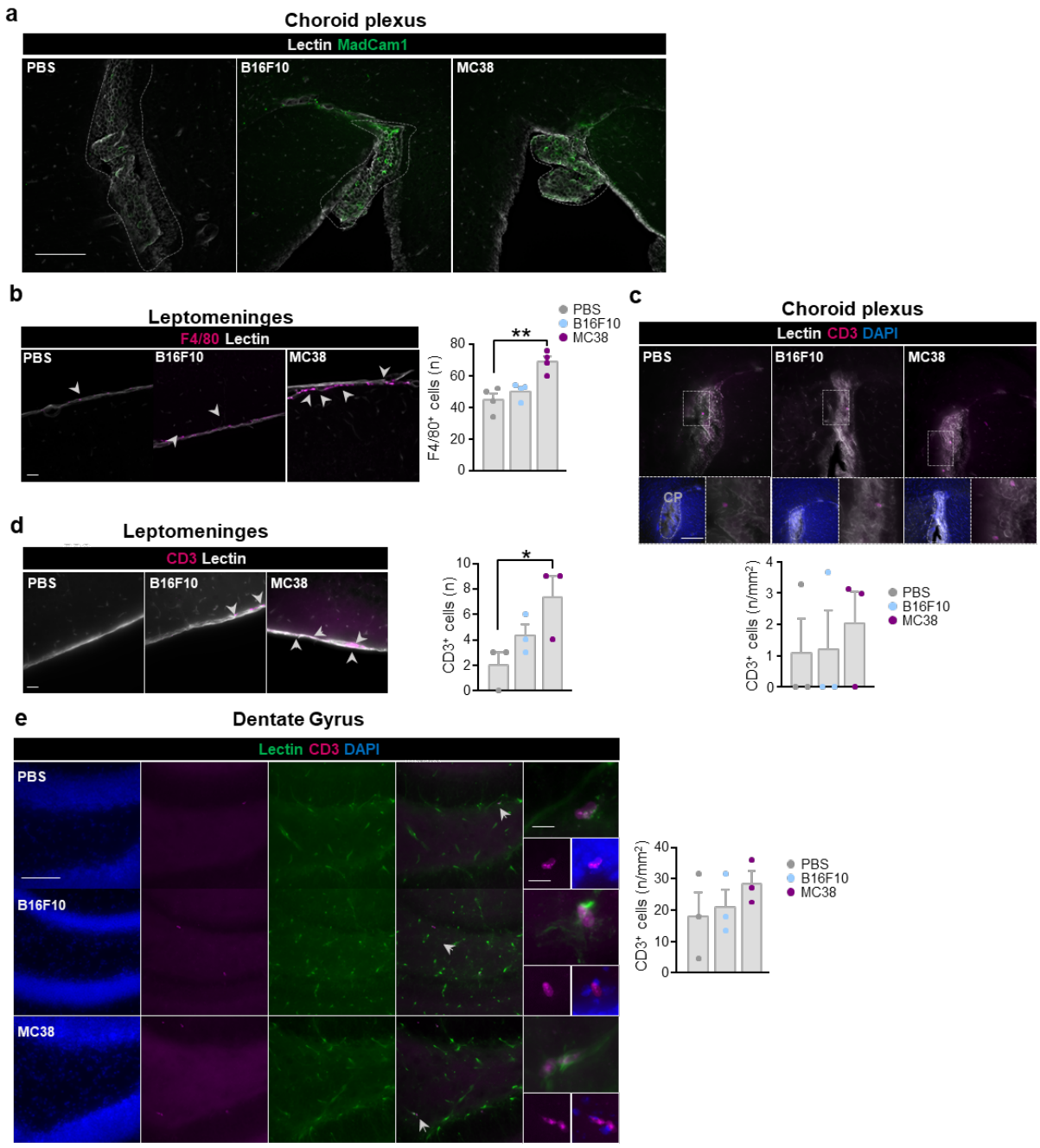

Figure S2. Neuroinflammation in choroid plexus, leptomeninges and hippocampus in B16F10 and MC38 tumor-bearing mice. a. Representative images of MadCam-1$^+$ (green) and Lectin$^+$ (grey) immunoreactivity in choroid plexus of PBS-control or B16F10 and MC38 mice. Scale bar: 100 µm. **b.** Representative images of Lectin (gray) and F4/80 (magenta) immunoreactivity in choroid plexus and leptomeninges of PBS-control or B16F10 and MC38 mice. Scale bar: 50 µm. Data are represented as bars with symbols for individual data points and they are expressed by mean ± SEM (=4), ** $p<0.01$. One-way ANOVA with Dunett's multiple comparisons test. **c.** Representative images and statistical quantification of the number of CD3+ TLs (CD3$^+$, magenta) in choroid plexus (Lectin$^+$, grey) of B16F10- and MC38-bearing mice compared to PBS-injected controls. Boxed areas represent lateral ventricular localization (DAPI, blue) of Lectin$^+$ cells and magnification of CD3$^+$ TLs (magenta). Right, bars indicate statistical comparison of number of TLs (n/mm^2, density) in B16F10- and MC38-mice compared to PBS-mice. Scale bar: 50 µm, zoom 10 µm. Data are represented as bars with symbols for individual data points and they are expressed by mean ± SEM (n=3), Kruskal-Wallis with Dunn's multiple comparisons test. **d.** Representative images and statistical quantification of number of T

lymphocytes ($CD3^+$, magenta) in leptomeninges ($Lectin^+$, grey) of B16F10- and MC38-bearing mice compared to PBS-injected controls. White arrows represent $CD3^+$ TLs (magenta). Right, bars indicate statistical comparison of number of TLs (n/mm^2, density) in B16F10- and MC38-mice compared to PBS-mice. Scale bar: 50 µm. Data are represented as bars with symbols for individual data points and they are expressed by mean ± SEM (n=3), * $p<0.05$. Kruskall-Wallis with Dunn's multiple comparisons test. **e.** Representative images of TLs ($CD3^+$, magenta) cells, vessels (Lectin+, green) and cells nuclei (DAPI, blue immunoreactivity) in dentate gyrus of PBS and B16F10- and MC38-bearing mice. Bottom, histogram bars indicate statistical comparison of number of CD3+ TLs (n/mm^2, density) in B16F10- and MC38-mice compared to PBS-mice. Scale bars: 100 µm, zooms 50 µm and 10 µm. Data are expressed by mean ± SEM (n=3). One-way ANOVA with Dunnett's multiple comparisons test.

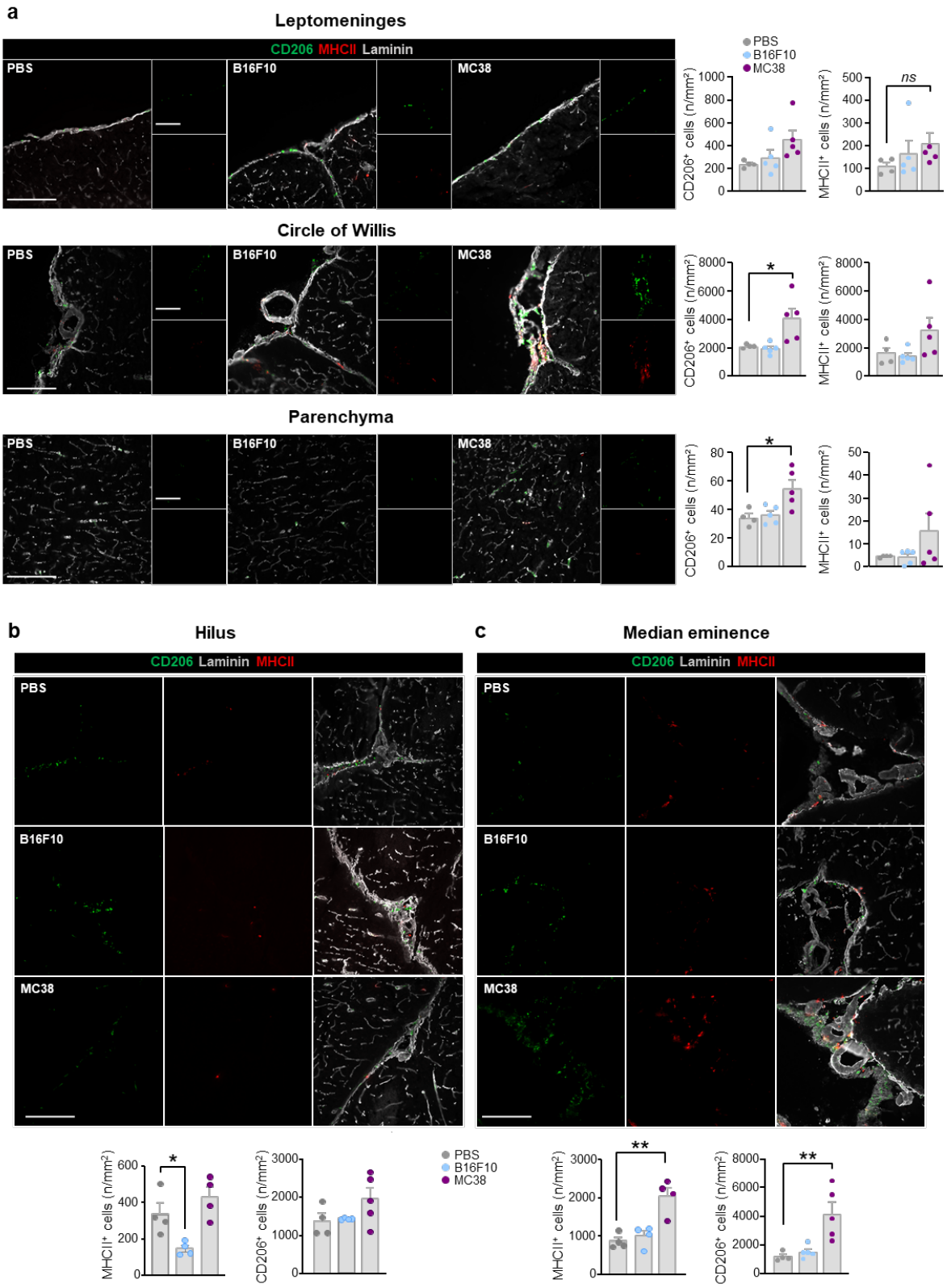

Figure S3. Peripheral cancers are associated with myeloid cells in circumventricular organs of cancer-bearing mice. Representative images and statistical quantification of density (n/mm^2) of pro-tumoral (CD206$^+$, green) and anti-tumoral (MHCII$^+$, red) myeloid cells staining in perivascular and vascular Laminin$^+$ spaces (grey) of the leptomeninges, circle of Willis and Parenchyma (**a**), hilus (**b**) and median eminence (**c**) of B16F10- and MC38-bearing mice compared to PBS-controls. Scale bar:

100 µm. Data are expressed as mean ± SEM (n=4-5), * $p<0.05$, ** $p<0.01$. ANOVA with Dunnett's or Kruskal-Wallis with Dunn's multiple comparisons test.

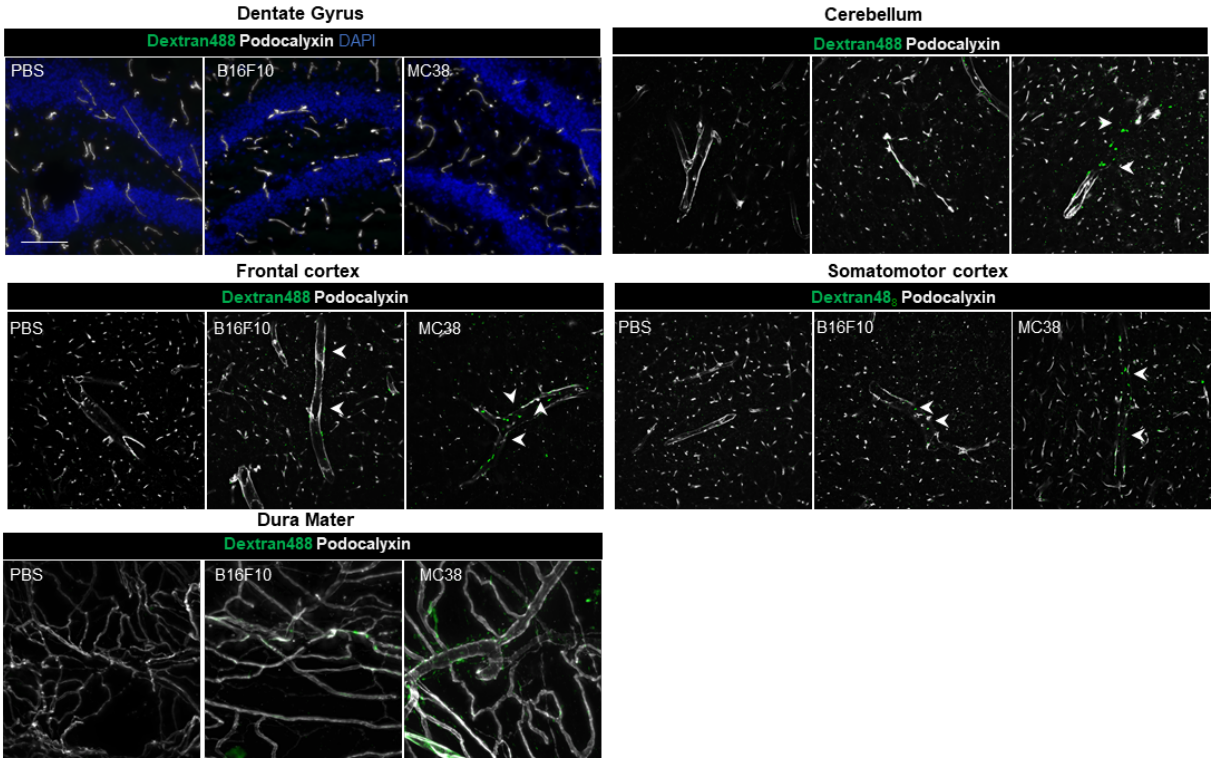

Figure S4. Peripheral cancers are associated with blood-brain barrier permeability. Representative microphotography showing $Dextran_{488}$ (green) extravasation from $Podocalyxin^{+}$ (grey) vessels in the dentate gyrus (upper panel, left), cerebellum (upper panel right), frontal cortex (lower panel, left), somatomotor cortex (lower panel, right), and the meningeal dura mater (lower left panel) of PBS and B16F10- and MC38-bearing mice. Scale bar: 50 μm.

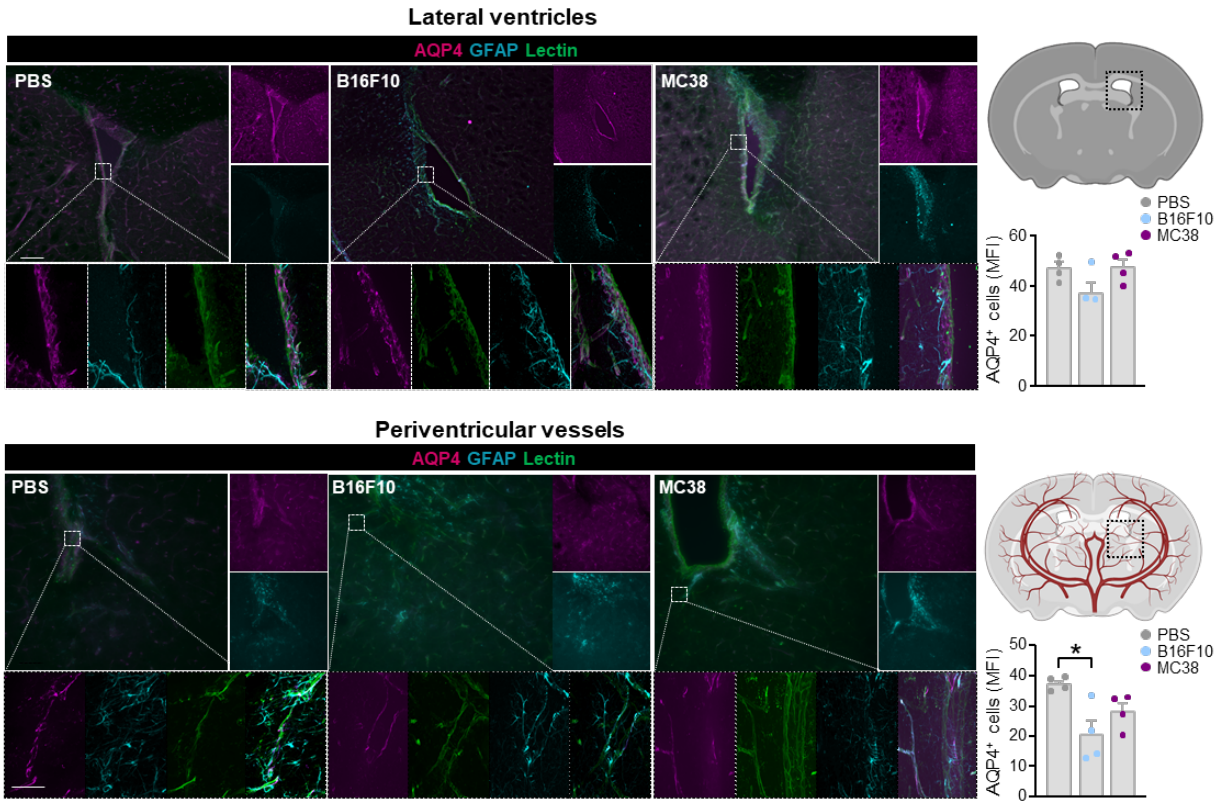

Figure S5. Aquaporin 4 in lateral ventricles and perivascular vessels in B16F10 and MC38-cancer-bearing mice. Upper panel, representative immunolabeling of Lectin$^+$ (green) vessels, AQP4$^+$ (magenta) and GFAP$^+$ (cyan) astrocytes in lateral ventricles of PBS, B16F10- and MC38 mouse brain slices. Boxed areas show magnification of AQ4$^+$GFAP+ astrocytes. Lower panel, representative immunolabeling of Lectin$^+$ periventricular vessels (green), AQP4$^+$ (magenta) and GFAP$^+$ (cyan) astrocytes of PBS, B16F10 and MC38 mouse brain slices. Boxed areas show magnification of AQP4$^+$GFAP+ astrocytes of Lectin$^+$ vessels. Right, histogram bars of quantification of AQP4 staining intensity expressed as median fluorescence intensity (MFI) in PBS, B16F10 and MC38 lateral ventricles and periventricular vessels. Scale bars: 200 µm, zoom 10 µm. Data are expressed as mean ± SEM (n=4), * $p<0.05$. One-way ANOVA with Dunnett's multiple comparisons test.

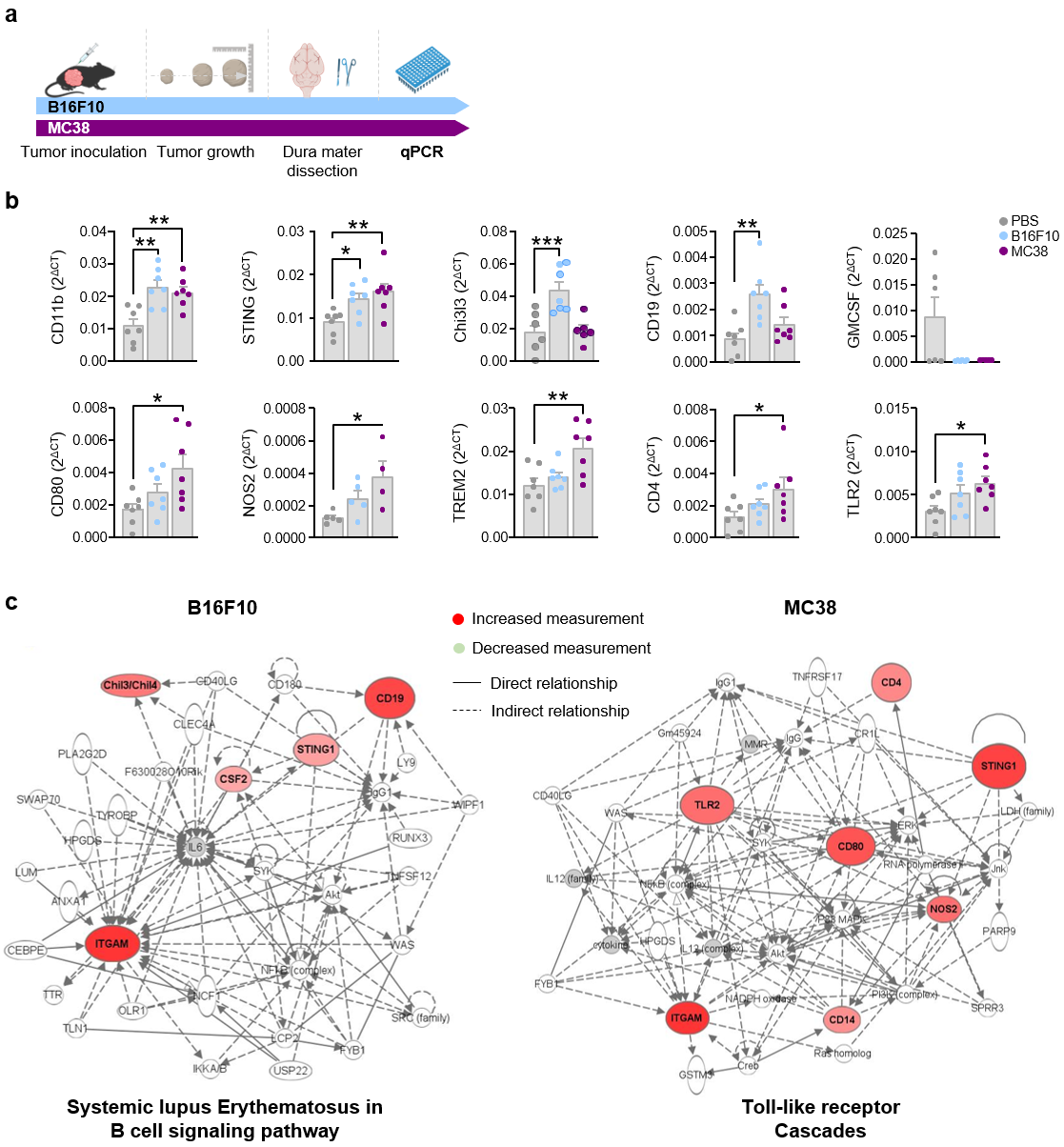

Figure S6. Peripheral cancers are associated with inflammation in the Dura Mater meningeal layer. a. Schematic diagram showing the timeline for dura mater isolation and qPCR analysis of inflammatory genes transcripts (n=48) in B16F10- (light blue) and MC38- (pink) bearing mice. **b.** Bars representing the statistical comparison of mRNA transcript levels expression of CD11b, STING, Chi3l3, CD19, GM-CSF, CD80, Nos2, CD4, TLR2 and TREM 2 in meningeal dura mater isolated from PBS, and B16- and MC38-bearing mice. Data are expressed as mean ± SEM (n=6-7), * $p<0.05$, ** $p<0.01$. One-way ANOVA with Dunnett's or Kruskal-Wallis with Dunn's multiple comparisons test. **c**. Gene interaction network maps generated by the Ingenuity Pathway Analysis (IPA) software representing one of the five canonical significant pathways from B16 (left) and MC38 (right) mice. In red, significant increased genes in each network.

a Differential analysis of selected genes in meninges of B16F10 *vs* PBS mice by Ingenuity pathway

Top Canonical pathways (PBS *vs* B16F10)		
Name	p-value	Overlap
Systemic lupus Erythematosus in B Cell Signaling Pathway	1.63E-04	0.6% (3/508)
Cgas-Sting Signaling Pathway	3.87E-04	1.6% (2/124)
IL-17 Signaling	6.19E-04	1.3% (2/157)
IL-12 Signaling and Production in Macrophages	1.06E-03	1.0% (2/206)
Pathogen Induced Cytokine Storm Signaling Pathway	2.46E-03	0.6% (2/315)
Top Disease and Bio Functions		
Diseases and disorders		
Name	p-value range	# molecules
Inflammatory Response	4.43E-02 – 6.06E-07	5
Infectious Disease	2.48E-02 – 6.12E-07	4
Organismal Injury and Abnormalities	4.74E-02 – 6.12E-07	5
Dermatological Disease	1.64E-02 – 1.55E-06	4
Connective tissue disorders	2.86E-02 – 2.46E-06	3
Molecular and Cellular Functions		
Name	p-value range	# molecules
Cellular Mouvement	3.33E-02 – 2.58E-08	5
Cell-To-Cell Signaling and Interaction	3.33E-02 – 1.02E-06	4
Cellular Development	4.82E-02 – 1.96E-06	4
Cellular Death and Survival	3.69E-02 – 1.05E-05	4
Cellular Compromise	2.38E-02 – 1.41E-05	4
Physiological System Development and Function		
Name	p-value range	# molecules
Hematological System Development and Function	4.84E-02 – 2.58E-08	5
Immune Cell Trafflicking	3.33E-02 – 2.58E-08	5
Tissue Morphology	4.04E-02 – 6.06E-07	5
Lymphoid Tissue Structure and Development	4.82E-02 – 1.96E-06	5
Connective Tissue Development and Function	4.80E-02 – 1.67E-05	4

b Differential analysis of selected genes in meninges of MC38 *vs* PBS mice by Ingenuity pathway

Top Canonical pathways (PBS *vs* MC38)		
Name	p-value	Overlap
Toll-Like Receptor Cascades	9.95E-08	10.3% (3/29)
MSP-RON Signaling Pathway	7.11E-07	5.5% (3/55)
Neutrophil Extracellular Trap Signaling Pathway	3.30E-06	1.1% (4/351)
Neutrophil Degranulation	7.95E-06	0.9% (4/438)
Defensins	9.80E-06	14.3% (2/14)
Top Disease and Bio Functions		
Diseases and disorders		
Name	p-value range	# molecules
Inflammatory Response	4.90E-02 – 1.20E-10	7
Infectious Disease	2.00E-02 – 2.97E-10	6
Organismal Injury and Abnormalities	4.96E-02 – 2.97E-10	7
Endocrine System Disorders	2.56E-02 – 3.65E-08	5
Gastrointestinal Disease	4.96E-02 – 3.65E-08	7
Molecular and Cellular Functions		
Name	p-value range	# molecules
Cell-To-Cell Signaling Interaction	4.32E-02 – 1.20E-10	7
Cellular Development	3.08E-02 – 1.50E-09	7
Cellular Growth and Proliferation	2.84E-02 – 1.50E-09	7
Cellular Function and Maintenance	3.80E-02 – 5.64E-09	7
Cell Death and Survival	4.39E-02 – 3.65E-08	7
Physiological System Development and Function		
Name	p-value range	# molecules
Hematological System Development and Function	4.56E-02 – 1.20E-10	7
Immune Cell Trafflicking	4.56E-02 – 1.20E-10	7
Organismal Survival	1.06E-03 – 2.59E-09	7
Tissue Morphology	4.39E-02 – 1.67E-08	7
Lymphoid Tissue Structure and Development	4.39E-02 – 6.37E-08	7

Figure S7. Signaling pathway enhanced in dura mater of cancer-bearing mice. Canonical pathway analysis, disease and function were studied by using the IPA system. The P-value of overlap <0.05 was set as the threshold and the significance level is obtained by Fisher's exact test at the right tail. IPA: ingenuity pathway analysis.

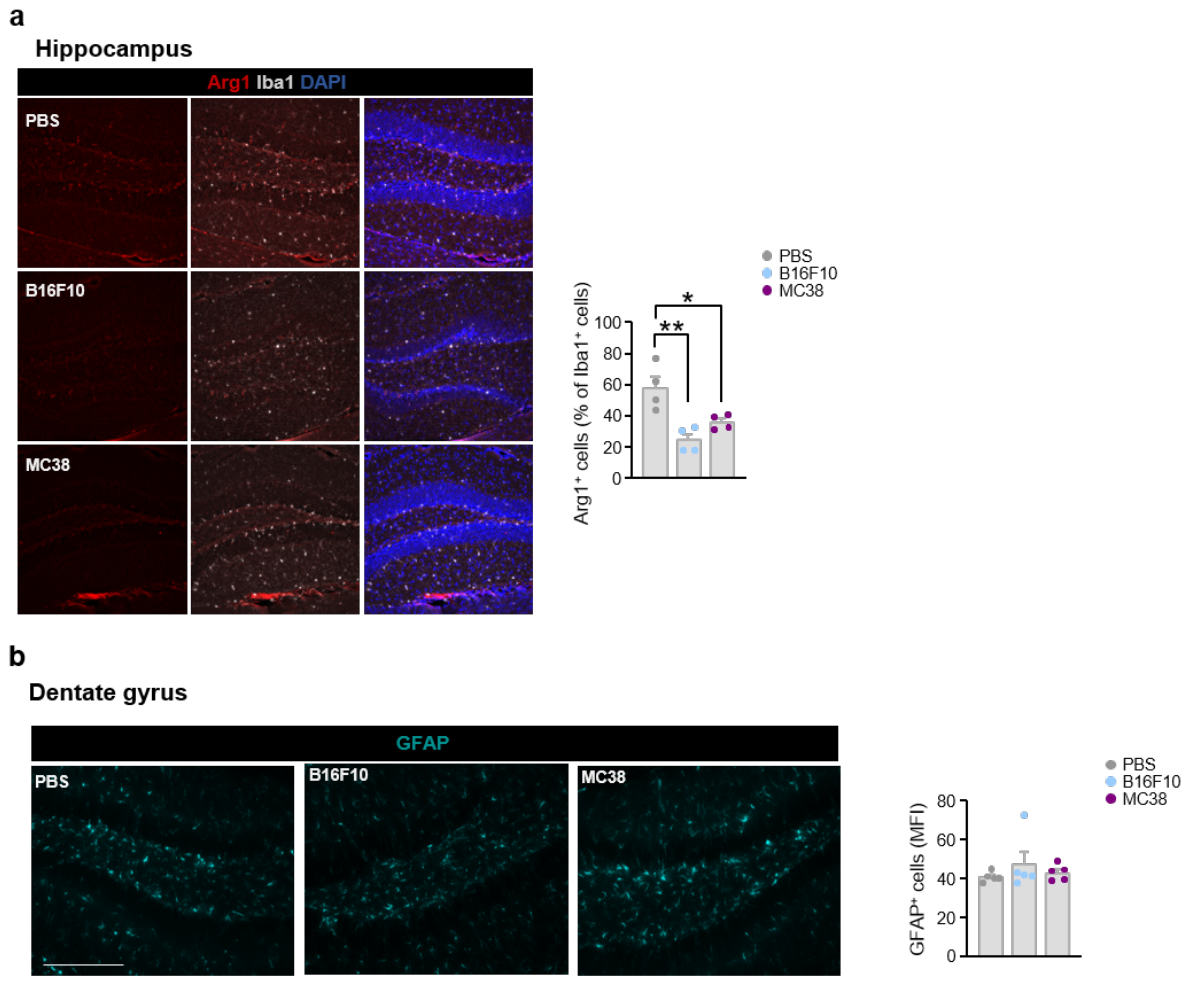

Figure S8. Microglia reactivity in the hippocampus of B16F10- and MC38 cancer-bearing mice. a. Immunofluorescence and statistical quantification of anti-inflammatory (Arg-1$^+$, red) microglial cells (Iba1$^+$, grey) in dentate gyrus (DAPI, blue) of B16F10- and MC38- bearing mice compared to PBS-mice. Scale bar: 100 µm. Data are expressed as mean ± SEM (n=4), * $p<0.05$, **$p<0.01$. One-way ANOVA with Dunnett's multiple comparisons test. **b.** Immunofluorescence of GFAP (n/mm^2, cyan) in dentate gyrus (DAPI, blue) of B16F10- and MC38- bearing mice compared to PBS-mice. Scale bar: 100 µm. Data are expressed as mean ± SEM (n=5). One-way ANOVA with Dunnett's multiple comparisons test.

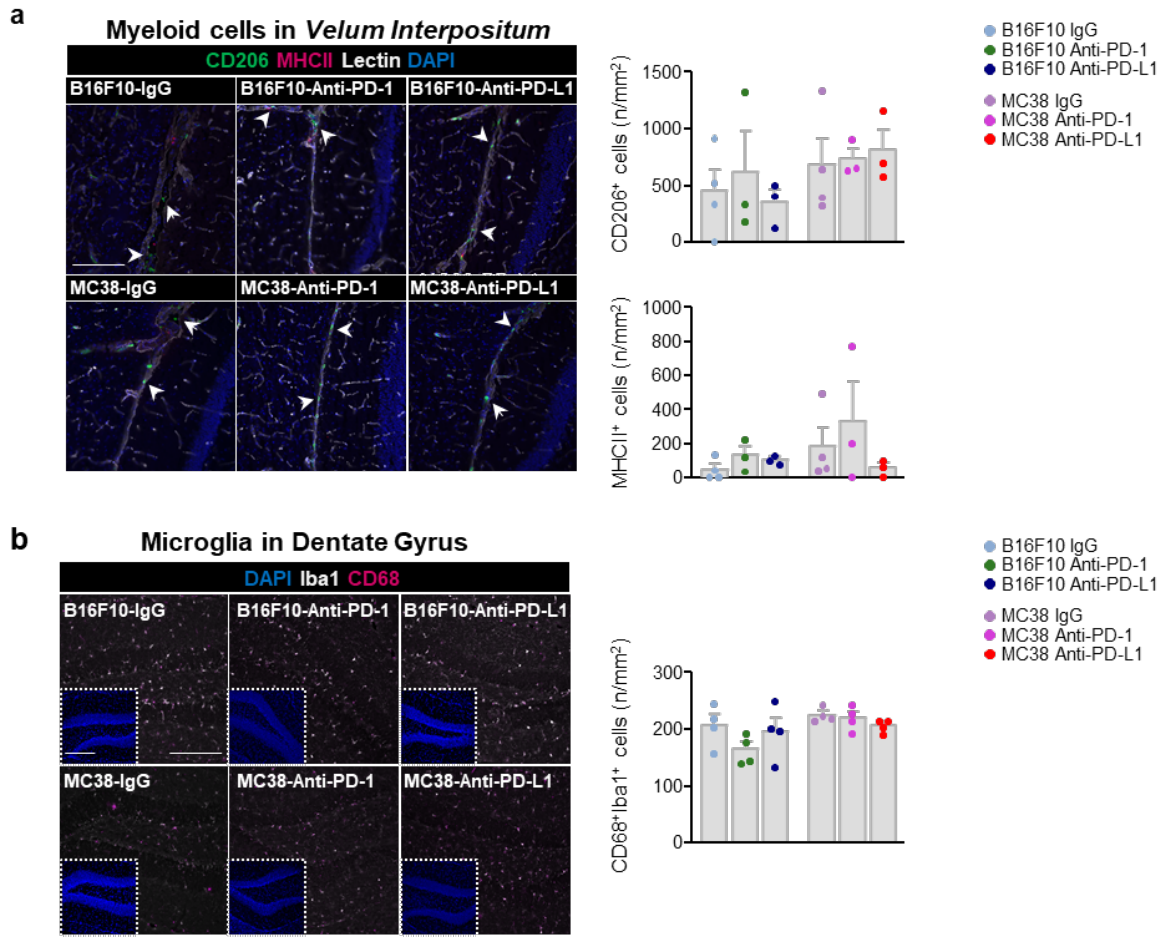

Figure S9. Quantification of myeloid cells in circumventricular organs of cancer-bearing mice. a. Immunofluorescence and statistical quantification of density (n/mm^2) of pro-tumoral (CD206$^+$) and anti-tumoral (MHCII$^+$) myeloid cells staining in perivascular and vascular Lectin$^+$ spaces (grey) of *Velum Interpositum* (left) of PBS-, B16F10- and MC38-bearing mice treated with anti-PD-1, anti-PD-L1 or IgG. Scale bar: 100 µm. Data are expressed as mean ± SEM (n=3-4), One-way ANOVA with Dunnett's multiple comparisons test. **b.** Immunofluorescence and statistical quantification of microglial cells (Iba1$^+$, grey and CD68, magenta) in dentate gyrus (DAPI, blue) of PBS-, B16F10- and MC38- bearing mice treated with anti-PD-1, anti-PD-L1 or IgG. Scale bar: 100 µm. Data are expressed as mean ± SEM (n=4), One-way ANOVA with Dunnett's multiple comparisons test.

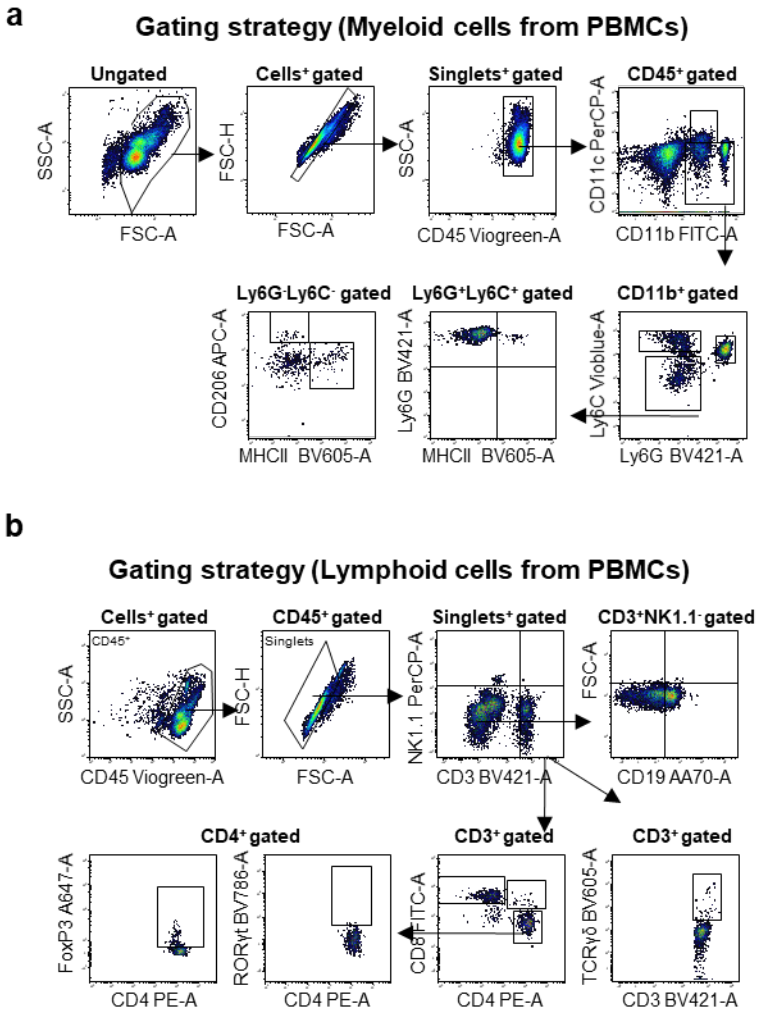

Figure S10. Gating strategy for the analysis of peripheral blood immune cells by flow cytometry from B16F10- and MC38-bearing mice. a. For myeloid panel, live cells were gated from FSC-A and SSC-A, singlets were gated from FSC-A and FSC-H, CD45 was used to identify leucocytes ($CD45^+$). From these cells, CD11c and CD11b were used to identify dendritic cells ($CD11c^+CD11b^+$) and monocytes ($CD11c^-CD11b^+$). From $CD11b^+$ cells, Ly6C, Ly6G and MHCII were used to identify macrophages ($CD11b^+Ly6C^-Ly6G^-$), neutrophils ($CD11b^+Ly6G^+Ly6c^-MHCII^-$), pro-tumoral macrophages ($CD11b^+Ly6C^-Ly6G^-$CD206+), anti-tumoral macrophages ($CD11b^+Ly6C^-Ly6G^-MHCII^+$), M-MDSCs ($CD11b^+Ly6G^-Ly6c^{high}$), PMN-MDSCs ($CD11b^+Ly6G^+Ly6C^{low}MHCII^+$). **b.** For lymphocytic panel, live cells were gated from FSC-A and SSC-A, singlets were gated from FSC-A and FSC-H, CD45 was used to identify leucocytes ($CD45^+$). From these cells, CD3 and NK1.1 were used to identify lymphocytes ($CD3^+NK1.1^-$) and NK cells ($CD3^-NK1.1^+$). From $CD3^+NK1.1^-$ cells, CD4 and CD8 were used to identify CD4 T cells ($CD4^+CD8^-$) and CD8 T cells ($CD8^+CD4^-$) and CD19 was used to identify B cells ($CD19^+$). From $CD3^+$ cells, TCRγδ cells were identify by using TCRγδ ($CD3^+TCR\gamma\delta^+$). From $CD4^+$ cells, FoxP3 and RORγT were used to identify Treg cells ($FoxP3^+CD3^+CD4^+$) and Th17 cells ($CD3^+CD4^+ROR\gamma T^+$).

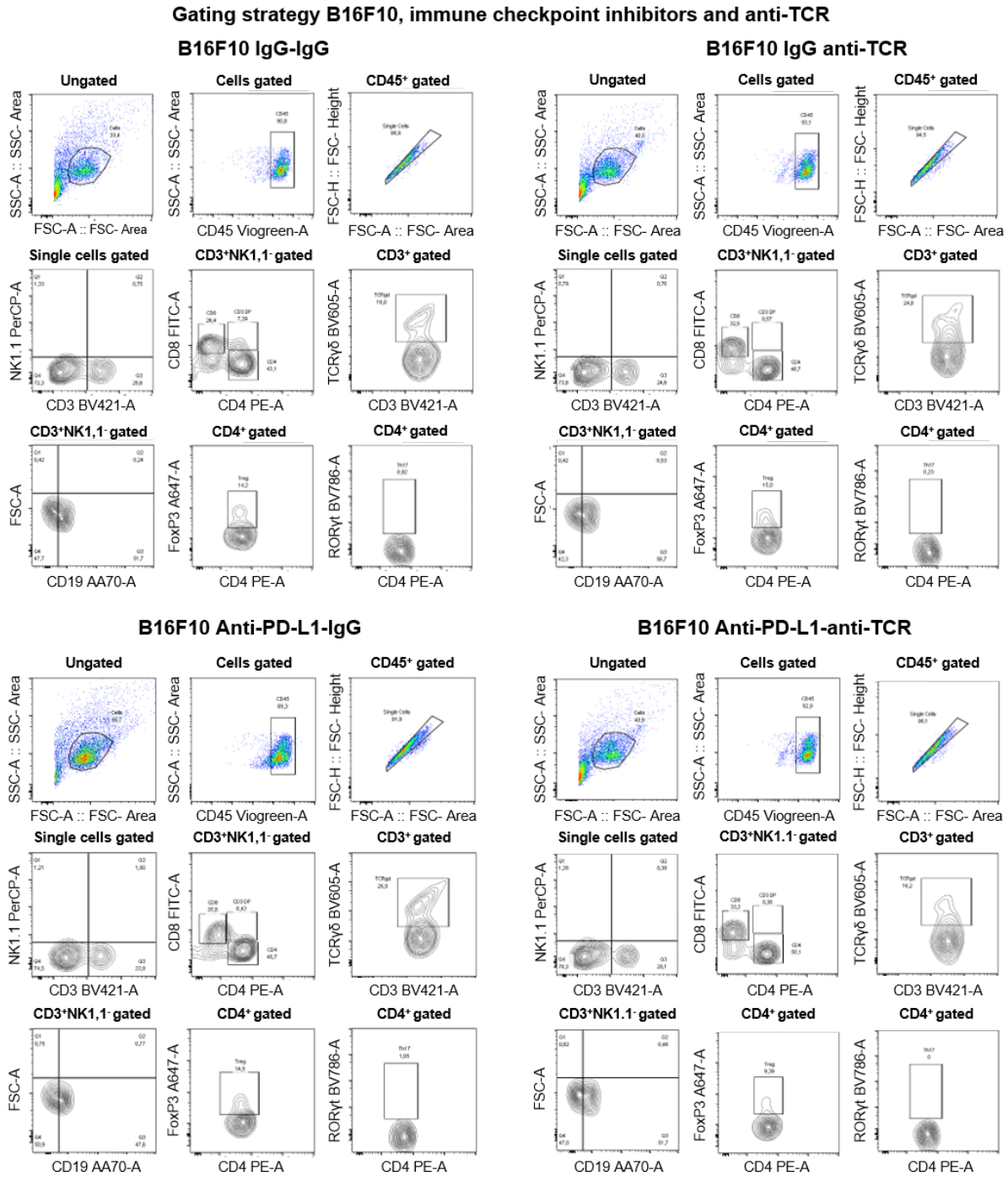

Figure S11. Gating strategy for the analysis of peripheral blood cells by flow cytometry from B16F10-bearing mice treated with anti-PD-L1 and/or anti-TCRγδ. Live cells were gated from FSC-A and SSC-A, singlets were gated from FSC-A and FSC-H, CD45 was used to identify leucocytes ($CD45^+$). From these cells, CD3 and NK1.1 were used to identify lymphocytes ($CD3^+NK1.1^-$) and NK cells ($CD3^-$, $NK1.1^+$). From $CD3^+NK1.1^-$ cells, CD4 and CD8 were used to identify CD4 T cells ($CD4^+CD8^-$) and CD8 T cells ($CD8^+CD4^-$) and CD19 was used to identify B cells ($CD19^+$). From $CD3^+$ cells, TCRγδ cells were identify by using TCRγδ ($CD3^+TCR\gamma\delta^+$). From $CD4^+$ cells, FoxP3 and RORγT were used to identify Treg cells ($FoxP3^+CD3^+CD4^+$) and Th17 cells ($CD3^+CD4^+ROR\gamma T^+$).

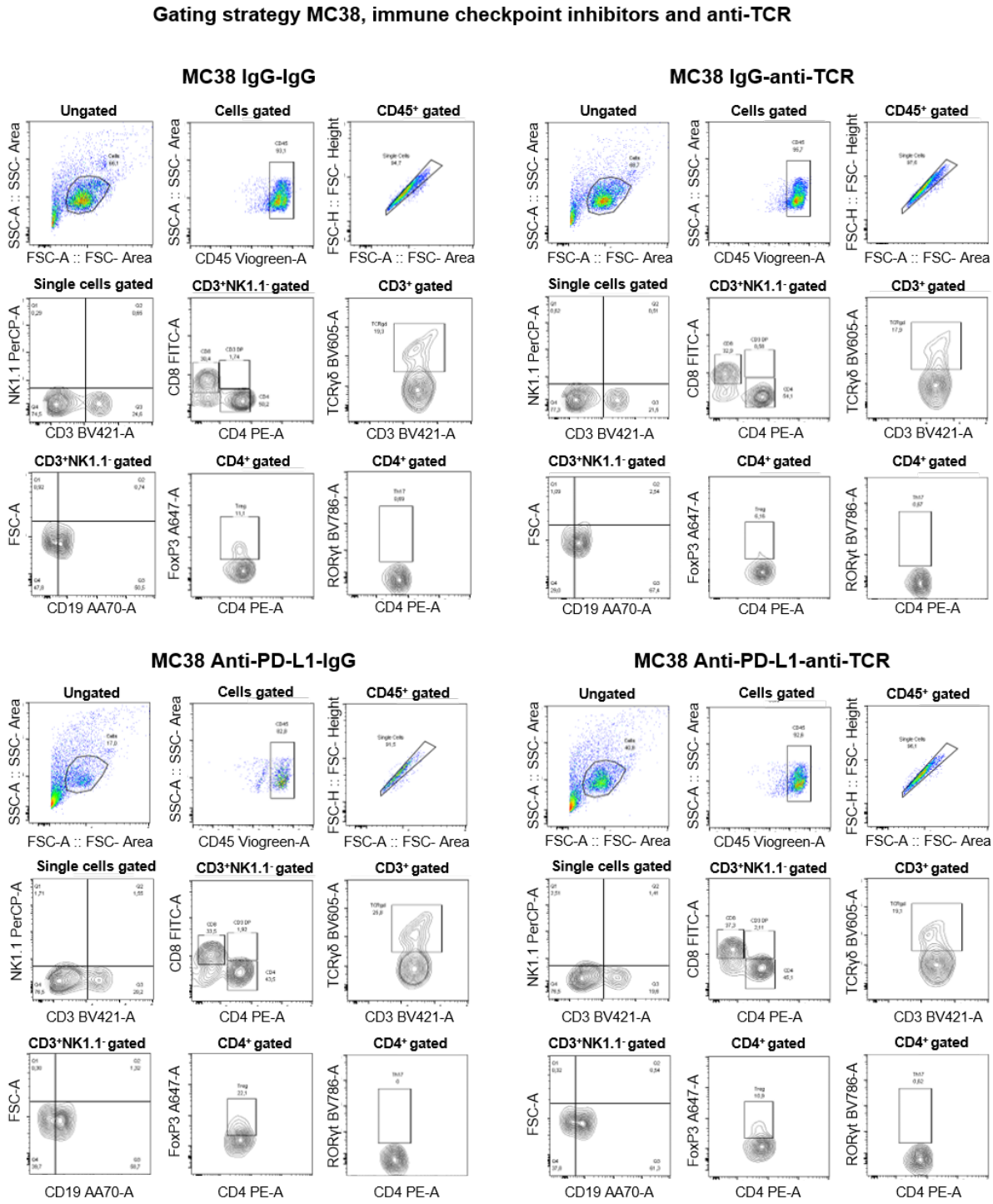

Figure S12. Gating strategy for the analysis of peripheral blood cells by flow cytometry from MC38-bearing mice treated with anti-PD-L1 and/or anti-TCRγδ. Live cells were gated from FSC-A and SSC-A, singlets were gated from FSC-A and FSC-H, CD45 was used to identify leucocytes ($CD45^+$). From these cells, CD3 and NK1.1 were used to identify lymphocytes ($CD3^+NK1.1^-$) and NK cells ($CD3^-$, $NK1.1^+$). From $CD3^+NK1.1^-$ cells, CD4 and CD8 were used to identify CD4 T cells ($CD4^+$, $CD8^-$) and CD8 T cells ($CD8^+$, $CD4^-$) and CD19 was used to identify B cells ($CD19^+$). From $CD3^+$ cells, TCRγδ cells were identify by using TCRγδ ($CD3^+TCR\gamma\delta^+$). From $CD4^+$ cells, FoxP3 and RORγT were used to identify Treg cells ($FoxP3^+CD3^+CD4^+$) and Th17 cells ($CD3^+CD4^+ROR\gamma T^+$).

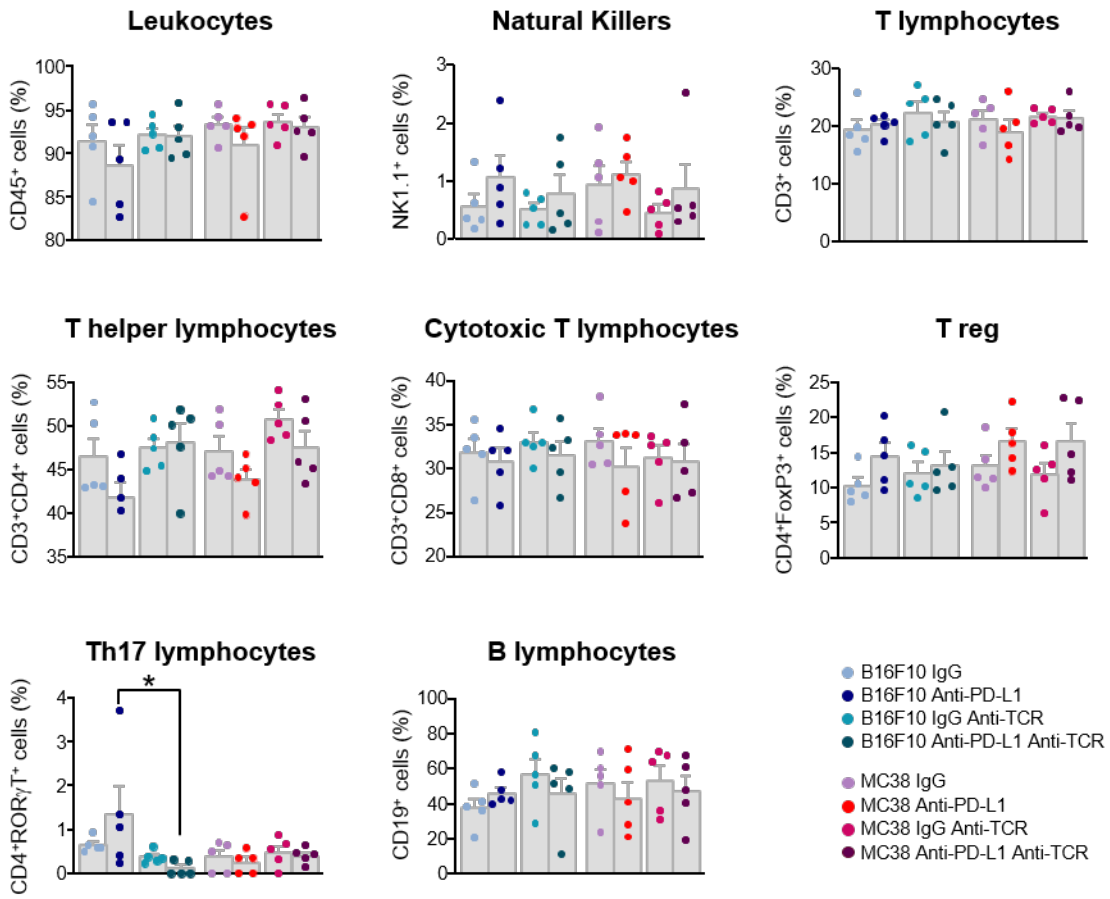

Figure S13. Impact of anti-TCRγδ on circulating immune cells of cancer-bearing mice treated with IgG, anti-PD1 or anti-PD-L1. Impact of anti-TCRγδ administration on the proportion of circulating $CD45^+$ leucocytes, $CD3^+$-$NK1.1^+$ NK cells, $CD3^+$ TLs, $CD3^+CD4^+$ T helper lymphocytes, $CD3^+CD8^+$ T cytotoxic Lymphocytes, $CD3^+CD4^+FoxP3^+$ Treg cells, double positive $CD4^+CD8^+$ TLs, $CD4^-CD19^+$ B cells and $CD3^+CD4^+RORγT^+$ Th17 cells in blood of B16F10- and MC38-bearing mice treated with anti-PD-L1 and IgG. Data are expressed as mean ± SEM (n=4-5), * $p<0.05$. One-way ANOVA with Sidak's multiple comparisons test.

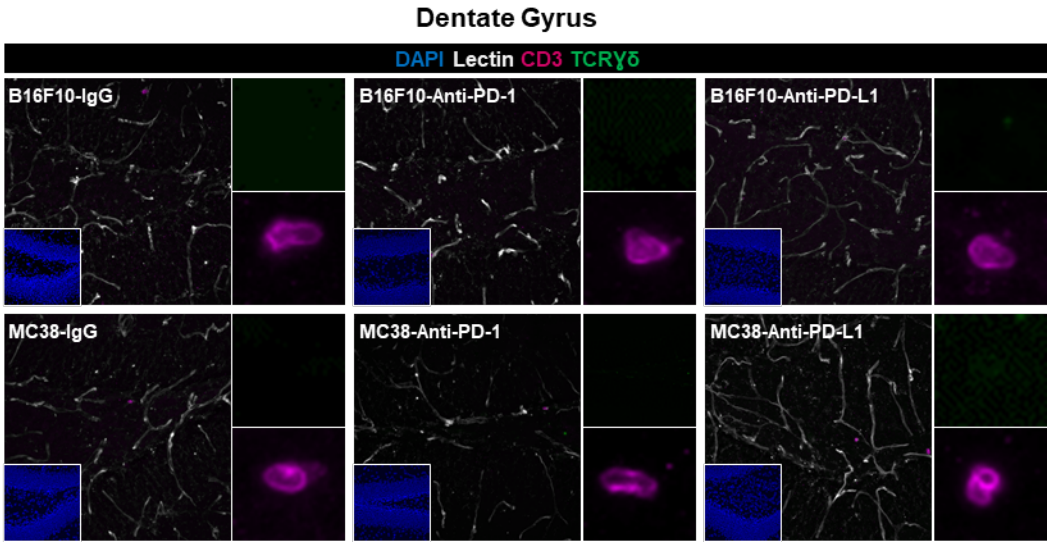

Figure S14. γδT lymphocytes infiltration in the hippocampus of cancer-bearing mice. Representative images of CD3 TILs (magenta), TCRγδ (green), Lectin (grey) and DAPI (blue) immunoreactivities in dentate gyrus of B16F10 or MC38-bearing mice treated with anti-PD-1, anti-PD-L1 or IgG. Scale bars: 50 µm, zoom 10 µm.